P364

Submitted to IEEE Journ. Quant. Electronics
appeared in Dec. 1986
QE-22 2224 (1986)

DYNAMICS OF THERMALLY INDUCED OPTICAL BISTABILITY

Istvan Janossy, J.Gordon H. Mathew, Eitan Abraham, Mohammad R. Taghizadeh

and S.Desmond Smith

Department of Physics, Heriot-Watt University, Riccarton,

Edinburgh EH14 4AS, U.K.

Abstract

The steady-state model of thermally induced optical bistability, presented in a previous paper, is extended to describe transient phenomena. A nonlinear integral equation is derived which can be readily solved for arbitrary time dependence of the input power. We apply the model to switching processes in bistable ZnSe interference filters. The corresponding experimental results are found to be in good agreement with the theoretical predictions.

1. Introduction

Recently thermally induced optical bistability has gained increasing interest. Devices based on thermal optical nonlinearities have from the point of view of applications attractive features, such as room temperature operation by cw laser beams and relative simplicity of fabrication. A prototype of these devices is the ZnSe interference filter, described in earlier papers [1,2,3,4]. It was demonstrated recently by us that the interference filter can be used as the basic switching element in optical circuits [5] which are necessary for all-optical computing.

In a previous paper ([4], from now on referred to as I.) we discussed a simple model of devices based on thermal optical bistability and compared it with experimental observations in interference filters. The model provided a good qualitative and reasonable quantitative agreement with the experimental results. In that paper only the steady state characteristics of the device were considered. However, from the point of view of applications it is also very important to study transient phenomena which is the aim of the present paper. We extend the model to non-stationary cases and compare the theoretical results with the experiments.

In section 2 we describe the model in detail. As in I. we consider a thin absorbing layer evaporated on a thick transparent substrate. We derive a nonlinear integral equation for the time dependence of the spot temperature T_s, i.e. the temperature at the centre of the laser beam. This equation can be readily solved numerically for arbitrary time-dependence of the incident power P. In the present paper we discuss in more detail the case of a stepwise increase or decrease of P from some P_L to $P_H = P_L + \Delta P$. In section 3 we describe the corresponding experimental results in ZnSe interference filters.

We focus our attention on switching processes, namely the transition from one branch of the bistable curve to the other, caused by a change in the input intensity. The switching process in our system can be divided into three parts. In the first time interval the spot temperature rises (or decreases) from the initial temperature, T_L, to the critical temperature at which the transition occurs. We refer to this time interval as the critical time, τ_c. In the next interval, the spot temperature passes through the unstable region (negative slope branch). Finally in the third interval the spot temperature is again in a stable region and approaches gradually its final stationary value T_H.

In section 3 we present experimental results on the switching process for different P_H values (for up-switching). In the experiments a long delay time was observed during which the transmission increased only slightly; this was followed by the actual switch, resulting in a rapid increase of the transmission. We demonstrate that the experimentally observed delay time is approximately twice that of the critical time, τ_c.

We found that as P_H approaches the switch-up threshold P_u, the delay time diverges. From our model we derive a simple approximation for the delay time, that accounts for the observed divergence (analogous to the critical slowing down phenomenon in phase transitions). Furthermore it emerges that the switching time is proportional to the square of the laser beam radius, provided that P_L/P_u and P_H/P_u are kept constant. Our experimental results are in good agreement with the above prediction.

In section 4 we discuss the implications of our results on device applications.

II. Theoretical Considerations

We consider a thin absorbing layer, evaporated on a thick transparent substrate. The time dependent heat flow equation is

$$c_i \rho_i \frac{\partial T}{\partial t} = Q(\underline{r},t) + \kappa_i \nabla^2 T \qquad (1)$$

where the index i = 1,2 refers to the layer and the substrate respectively. $Q(\underline{r},t)$ is the quantity of heat absorbed/unit volume/unit time at the position $\underline{r}$ at the time t. $Q(\underline{r},t)$ is zero for the substrate, while for the layer

$$Q(\underline{r},t) = I(\underline{r},t)\ \alpha\ (T(\underline{r},t)) \qquad (2)$$

where I is the irradiance and α is the absorption coefficient. As we deal with pure thermal effects we assume that α is a function of the local temperature only.

As in I., we consider the case when the material parameters (c,ρ,κ) in eqn. (1) are equal for the two media. We neglect heat transfer to the air and consider the substrate to be semi-infinite. The boundary conditions are the same as in the steady state case: the normal component of the heat current is zero at the layer-air interface (z = 0 plane) and at large distances from the absorbing spot the temperature approaches the ambient temperature T_F. Using the Green function technique, eqn. (1) can be converted into an integral form:

$$T(\underline{r},t) - T_F = \frac{D}{\kappa} \int_{-\infty}^{t} \int_{\underline{r}'} \frac{Q(\underline{r}',t')}{(4\pi D(t-t'))^{3/2}} \exp\left(-\frac{(\underline{r}-\underline{r}')^2}{4D(t-t')}\right) d^3\underline{r}'dt'$$

. . . . . (3)

where $D = \kappa/c\rho$ is the thermal diffusivity. The spatial part of the integration is over the irradiated spot and includes the "mirror sources" too, which are obtained by reflecting the real heat sources on the $z = 0$ plane.

Using the same considerations as in I., in the limit of very thin layers eqn. (3) becomes

$$T(\underline{\rho},t) - T_F = \frac{2D}{\kappa} \int_{-\infty}^{t} \int_{\rho'} \frac{I_{in}(\rho',t')\, A\,(T(\rho',t'))}{(4\pi D(t-t'))^{3/2}} \exp\left(-\frac{(\underline{r}-\underline{r}')^2}{4D(t-t')}\right) d\underline{\rho}'dt' \qquad \ldots\ldots (4)$$

where $\underline{\rho}$ is a position vector in the $z = 0$ plane and $I_{in}(\underline{\rho}',t')$ is the irradiance of the incident beam at $\underline{\rho}'$. For a Gaussian beam with $1/e^2$ radius ρ_0

$$I_{in}(\rho',t') = \frac{P(t')}{\pi\rho_0^{\,2}}\, e^{-\rho'^2/\rho_0^{\,2}} \qquad (5)$$

A(T) is the absorptance of the layer, i.e. the fraction of the input intensity which is absorbed in the layer at a fixed temperature T. We note that although in the absence of absorption ($\alpha = 0$) the absorptance is necessarily zero, in general A(T) is not determined unambiguously by α. The reason for this is that the amount of absorption within the layer is strongly influenced by cavity effects which in turn depend critically on the refractive index n. A detailed discussion of this problem was given in I.

Eqn. (4) represents a complicated integral equation for the temperature distribution. A first approximation of the solution can be obtained by neglecting the spatial variation of the temperature within the spot.

Replacing $A(T(\underline{\rho}',t'))$ by $A(T_s(t'))$, where T_s is the temperature at the centre of the beam, we obtain for a Gaussian beam

$$T_s(t) - T_F = \frac{\tau_0^{1/2}}{2\rho_0\kappa\pi^{1/2}} \; \frac{2}{\pi} \int_{-\infty}^{t} \frac{P(t')\,A\,(T_s(t'))}{(t-t')^{1/2}\;(t-t'+\tau_0)}\,dt' \qquad (6)$$

with $\tau_0 = \rho_0^2/4D$.

For a constant incident power, P, eqn. (6) reduces to

$$T_s - T_F = P\,\frac{A(T_s)}{2\sqrt{\pi}\,\kappa\,\rho_0} \qquad (7)$$

Eqn. (7) was obtained already in Ref. I., and it was applied to calculate the steady state characteristics of the device. For bistability there are two critical points in the $P = P(T_s)$ curve at which $\partial P/\partial T_s = 0$. We refer to the critical temperatures as T_u and T_D; the corresponding powers are the switch-up power, P_u, and the switch-off power. In the temperature interval $T_u < T_s < T_D$ there is no stable stationary solution.

As mentioned in the introduction we are interested in the case when P is changed discontinuously from P_L to P_H, i.e.

$$P(t) = \begin{cases} P_L \text{ for } t < 0 \\ P_H \text{ for } t > 0 \end{cases} \qquad (8)$$

Inserting this form of P(t) into eqn. (6) we obtain for $t > 0$

$$T_s(t) - T_F = (T_L - T_F)\left(1 - \frac{2}{\pi} \arctan \sqrt{\frac{t}{\tau_0}}\right) + \frac{\tau_0^{1/2}}{2\rho_0 \kappa \pi^{1/2}} \frac{2}{\pi} P_H \int_0^t \frac{A(T_s(t'))}{(t-t')^{1/2}\,(t-t'+\tau_0)} dt' \tag{9}$$

Eqn. (9), which is the central result of this section, is an Abel-Volterra type of equation with a weakly divergent kernel. There are well established methods for the numerical solution of such equations [6]. To apply it to a specific system, the thermal data of the substrate and the temperature dependence of the absorptance of the active layer, A(T), must be known. Note that the input parameter is the initial spot temperature, T_L, rather than the initial power P_L. Outside the bistable power region there is a one-to-one correspondence between T_L and P_L; however if P_L is within the bistable range it has to be specified which state (on or off) is the system initially in. The solution of the problem is of course entirely different for the two initial conditions.

To discuss the spot size dependence of transient phenomena we introduce the dimensionless variable $s = t/\tau_0$. Eqn. (9) can be written as

$$T_s(t) - T_F = (T_0 - T_F)\left(1 - \frac{2}{\pi} \arctan\sqrt{s}\right) + \frac{P_1}{2\rho_0 \kappa \pi^{1/2}} \frac{2}{\pi} \int_0^s \frac{A(T(t'))}{(s-s')^{1/2}(s-s'+1)} ds' \tag{10}$$

From eqn. (10) it follows that providing P_L/ρ_0 and P_H/ρ_0 are kept constants T_s is a function of s only. This implies that the time required to achieve a certain temperature rise (or fall) is proportional to τ_0, which is in turn proportional to the square of the spot size, ρ_0^2 (see eqn. (6)).

The above consideration can be extended to general forms of P(t). Inserting into eqn. (6) $P(t) = p(t/\tau_0)/\rho_0$, it can be seen that the temperature rise is a function of $s = t/\tau_0$ and the form of the function P(s) only. This implies that by reducing the spatial scale (i.e. the spot size) by a given factor, reducing the power by the same factor and reducing the time scale by the square of this factor we obtain the same transient behaviour on these reduced scales.

III. Application of the Model to ZnSe Interference Filters

In this section we apply the theoretical model to a ZnSe interference filter evaporated on a glass substrate. The structure of the filter and some basic experimental observations of the nonlinear optical behaviour was given in [2]. Further experimental results were reported in I.

The basic experimental set-up used in the present experiments was similar to the previous ones, except for an acousto-optical modulator which was inserted into the beam path. The acousto-optical modulator (Coherent, Model 304) was controlled from a microcomputer. The incident laser power could be incremented between two levels in a time less than 5 μs. Both the incident and transmitted powers were monitored on a Tektronix 7633 storage scope, allowing the entire switching waveform to be observed. The ZnSe interference filter was the same used in the previous steady state experiments (I.); the light source was the 514.5 nm line of a Coherent Ar laser (Innova 10).

In Fig. 1 we show a set of experimental curves for the switch-up process. The initial power P_L was the same for all curves and the filter was held in the off state. The power was stepwise increased to $P_H > P_u$. As shown in the figure, there are simultaneous stepwise increases in the transmitted powers which correspond to no change in the transmission coefficients. There is a long period during which the transmission increases only slightly and this is followed by a rapid "switch". A very slight overshooting was observed in the transmission and the new equilibrium was established gradually.

In Fig. 2(a) we show the dependence of the switching time on P_H. We define the switching time as the time interval from the increment of the power until the moment when the transmission curve has an inflexion point. As can be seen from the figure, the switching time steeply increases as P_H/P_u gets close to unity (critical slowing down).

In order to carry out a corresponding theoretical analysis we need to know the temperature dependence of the absorptance and the thermal data (see eqn. (9)). The form of the function A(T) for the ZnSe filter was discussed in I. We demonstrated that near the resonance it can be approximated as

$$A(T) = \frac{A_0}{1 + G(\theta-\theta_0)} \qquad (11)$$

where θ is the angle of incidence of the laser beam. In the temperature range of interest for the present problem A_0, G and θ_0 can be regarded as linear functions of the temperature. For the filter on which we carried out our measurements we found (I.).

$$A_0 = A_1 + A_2\ (T-T_F) \qquad G = G_1 + G_2\ (T-T_F)$$

$$\theta_0 = \theta_1 + \theta_2\ (T-T_F)$$

with T_F = 20°C and

$$A_1 = .45 \qquad A_2 = -\ 0.01/°C$$

$$G_1 = .18 \qquad G_2 = -\ 0.0003/°C$$

$$\theta_1 = 30.5 \qquad \theta_2 = .055/°C$$

The transmission coefficient obeys a similar relation

$$\tau(T) = \frac{T_0}{1 + G(\theta-\theta_0)^2} \tag{12}$$

with $\qquad T_1 = .2 \qquad T_2 = -0.0007/°C$

In Fig. 3 we show the calculated spot temperature as a function of the time for a fixed P_L (P_L = .6 P_u) and for different values of P_H. The curves show clearly the three different time intervals, observed in the experimental results also. In the figure we indicate the critical temperatures T_u and T_D. As can be seen, there is first a long time interval during which the temperature rises almost linearly. The duration of this interval is roughly twice of the time necessary to raise the temperature to the first critical temperature T_u. In the second interval the temperature increases rapidly, within the unstable region, $T_u < T_s < T_D$. Finally the rate of the temperature rise decreases and equilibrium is reached gradually.

In Fig. 4 we present the transmission coefficients as a function of time. The transmission coefficient was calculated by using eqn. (12) replacing T by T_s. The general shape of the curves is similar to that of the experimental ones except for the fact the calculated overshootings are much more significant than the detected ones. The reason for this is the following. By using eqn. (12) we determine the transmission coefficient at the centre of the beam, while in the measurements the whole transmitted beam was collected on the detector. The peak in the calculated curve corresponds to the spot temperature at which the transmission coefficient is maximum ($\theta_0(T_s) = \theta$). However, because there is a temperature gradient across the spot, when the local transmission coefficient is maximum at the centre of the beam, the transmission coefficient of the total beam is significantly lower than this maximum. The overshooting, predicted for the centre of the beam is very much reduced by spatial effects.

In order to demonstrate that our model describes the observed critical slowing down, we estimate the critical time, τ_c, necessary to raise the temperature from its initial value, T_L to T_u. In this temperature range the absorptance A increases with increasing temperature. Consequently if $A(T_s(t'))$ is replaced by $A(T_u)$ in eqn. (9), the temperature rise will be overestimated. Hence we obtain the inequality

$$T_s(t) - T_F < (T_L - T_F)\left(1 - \frac{2}{\pi}\,\text{arc tan}\sqrt{\frac{t}{\tau_0}}\right) + \frac{P_H\,A(T_u)}{2\rho_0\kappa\pi^{1/2}}\,\frac{2}{\pi}\left(\text{arc tan}\sqrt{\frac{t}{\tau_0}}\right) \tag{13}$$

Rearranging the above inequality, we obtain for τ_c

$$\tau_c > \tau_0 \tan^2\left(\frac{\pi}{2}\,\frac{P_u A(T_u) - P_L A(T_L)}{P_H A(T_u) - P_L A(T_L)}\right) \tag{14}$$

where it was taken into account that by definition $T_s(\tau_c) = T_u$. We made use also of the relations

$$T_L - T_F = \frac{P_L A(T_L)}{2\rho_0 \kappa \pi^{1/2}} \quad , \quad T_u - T_F = \frac{P_u A(T_u)}{2\rho_0 \kappa \pi^{1/2}}$$

which follow from the steady state solution (eqn. (7)).

For $P_H \to P_u$ the r.h.s. of the inequality (14) diverges and as a consequence τ_c must diverge too. In fact for P_H only slightly larger than P_u the inequality becomes a good approximation. As we showed the switching time, τ_s, is roughly $2\tau_c$, so we obtain

$$\tau_s \approx 2\tau_0 \tan^2 \left(\frac{\pi}{2} \frac{P_u A(T_u) - P_L A(T_L)}{P_H A(T_u) - P_L A(T_L)}\right) \tag{15}$$

$$\text{for } 0 < \frac{P_H - P_u}{P_u} \ll 1$$

The switching time as a function of P_H, according to the above approximation is displayed in Fig. 2(b). The similarity to the experimental curve is obvious. A good quantitative agreement between the theoretical and experimental curves can be obtained in the region near to $P_H/P_u = 1$ (where the approximation is valid) by assuming $\tau_0 = 0.5$ msec. On the other hand, the relation $\tau_0 = \rho_0{}^2/4D$ with $\rho_0 = 50$ µm and $D = 1.76 \times 10^{-2}$ cm^2/sec (float glass) yields $\tau_0 = 0.36$ msec, in reasonable agreement with the value quoted above.

As can be seen from the curves in Fig. 3, the critical slowing down is due to the fact that as P_H approaches P_u, the temperature rise becomes slower and slower in the vicinity of the critical temperature T_u. This behaviour is a universal feature of bistable systems and is discussed in detail in [7,8,9].

In Fig. 5 we present the spot size dependence of the switching time. As pointed out in section 2 our model predicts quadratic dependence of the switching time (or any other transient time) on the spot size. This relation is confirmed by our measurements in a rather good approximation. The actual slope of the fitted straight line in Fig. 5 is 2.3. We note that the measurement of small spot sizes (ρ_0 10 μm) is rather inaccurate and this may explain the small deviation of the experimental and theoretical results. Furthermore, as pointed out in I. for the steady state case, for small spot sizes the replacement of the thermal constants, D and κ, by those of the substrate cannot be justified. This fact may lead to deviations from the quadratic law for small spot sizes.

IV. Conclusions

In the theoretical part of our paper we presented a nonlinear integral equation (eqn. (6)), which can be applied to describe the temperature variation in an absorbing thin film under the influence of a non-stationary input power. We applied this model to describe switching processes in nonlinear interference filters and compared the results with experimental observations.

From our study we draw the important conclusion that by decreasing the spot size both the critical switching power and the switching time decrease. Therefore for device application it seems desirable to work with the smallest possible spot sizes. The limitations are the following. Firstly it becomes increasingly difficult to produce Gaussian beams with diameters less than a few microns. Secondly with decreasing spot size the critical irradiance increases (in contrast to the critical power). Consequently the problem of photoinduced permanent changes becomes more serious. We also note that for spot sizes less than a few microns, the scaling laws established in section 2 do not necessarily hold. This point needs further investigation.

The characteristic time involved in the problem is $\tau_0 = \rho_0{}^2/4D$. For switching powers only slightly higher than the critical switching power, P_u, there is a delay time which is much longer than τ_0. However for $P_H \approx 2P_u$ the switching time is comparable with τ_0 (see Fig. 3). Assuming $\rho_0 = 5$ μm and $D = 1.76 \times 10^2$ cm^2/sec we obtain $\tau_0 = 3.6$ μsec. For many applications this may be an acceptable switching time. Thus we believe that thermally induced bistability, in spite of its relative slowness as compared to electronic nonlinearities, can find useful device applications.

References

[1] F.V. Karpushko and G.V. Sinitsyn, "The Anomalous Nonlinearity and Optical Bistability in Thin-Film Inteference Structures", Appl. Phys. B, vol. 28, 137 (1982); S.P. Apanasevich, F.V. Karpushko and G.V. Sinitsyn, "Response Time of Bistable Devices Based on Evaporated Thin-Film Interferometers", Sov. J. Quantum Electron., vol. 14 873-874 (1984).

[2] S.D. Smith, J.G.H. Mathew, M.R. Taghizadeh, A.C. Walker, B.S. Wherrett and A. Hendry, "Room Temperature Visible Wavelength Optical Bistability in ZnSe Interference Filters", Opt. Commun., vol. 51, 357-362 (1984).

[3] G.R. Olbright, N. Peyghambarian, H.M. Gibbs, H.A. MacLeod and F. Van Milligen, "Microsecond Room-Temperature Optical Bistability and Crosstalk Studies in ZnS and ZnSe Interference Filters with Visible Light and Milliwatt Powers", Appl. Phys. Lett., vol. 45, 1031-1033 (1984).

[4] I. Janossy, M.R. Taghizadeh, J.G.H. Mathew and S.D. Smith, "Thermally Induced Optical Bistability in Thin Film Devices", IEEE J. Quantum Electron., 21(9) (1985).

[5] S.D. Smith, I Janossy, H.A. MacKenzie, J.G.H. Mathew, J.J.E. Reid, M.R. Taghizadeh, F.A.P. Tooley and A.C. Walker, "Nonlinear Optical Circuit Elements as Logic Gates for Optical Computers: The First Digital Optical Circuits", Opt. Eng., vol. 24, 569-574 (1985).

[6] H.J.J. te Riele, IMA J. Numer. Anal., vol. 2 437 (1982).

[7] E. Garmire, J.H. Marburger, S.D. Allen and H.G. Winful, "Transient Response of Hybrid Bistable Optical Devices", Appl. Phys. Lett., vol. 34, 374-378 (1979).

[8] P. Mandel, "Nonlinear Stability of an Optical Transistor", Opt. Commun,., vol. 54, 181-184 (1985).

[9] H.A. Al-Attar, H.A. MacKenzie and W.J. Firth, "Critical Slowing Down Phenomena in an InSb Optical Bistable Etalon" to be published.

Figure Captions

Fig. 1 Transmitted powers as a function of time for different P_H/P_u ratios. Spot radius 50 μm, angle of incidence 40°.

Fig. 2 a) Experimental switching times as a function of P_H/P_u. Spot radius 50 μm, angle of incidence 40°.
b) Theoretical curves for switching times, according to eqn. (15).

Fig. 3 Calculated spot temperatures as a function of time, for diffrent P_H/P_u ratios. Angle of incidence 40°.

Fig. 4 Calculated transmission coefficients as a function of time for different P_H/P_u ratios. Angle of incidence 40°.

Fig. 5 Switching time as a function of the incident spot diameter. Angle of incidence 40°; $P_L = 0.6\ P_u$.

Fig. 1.

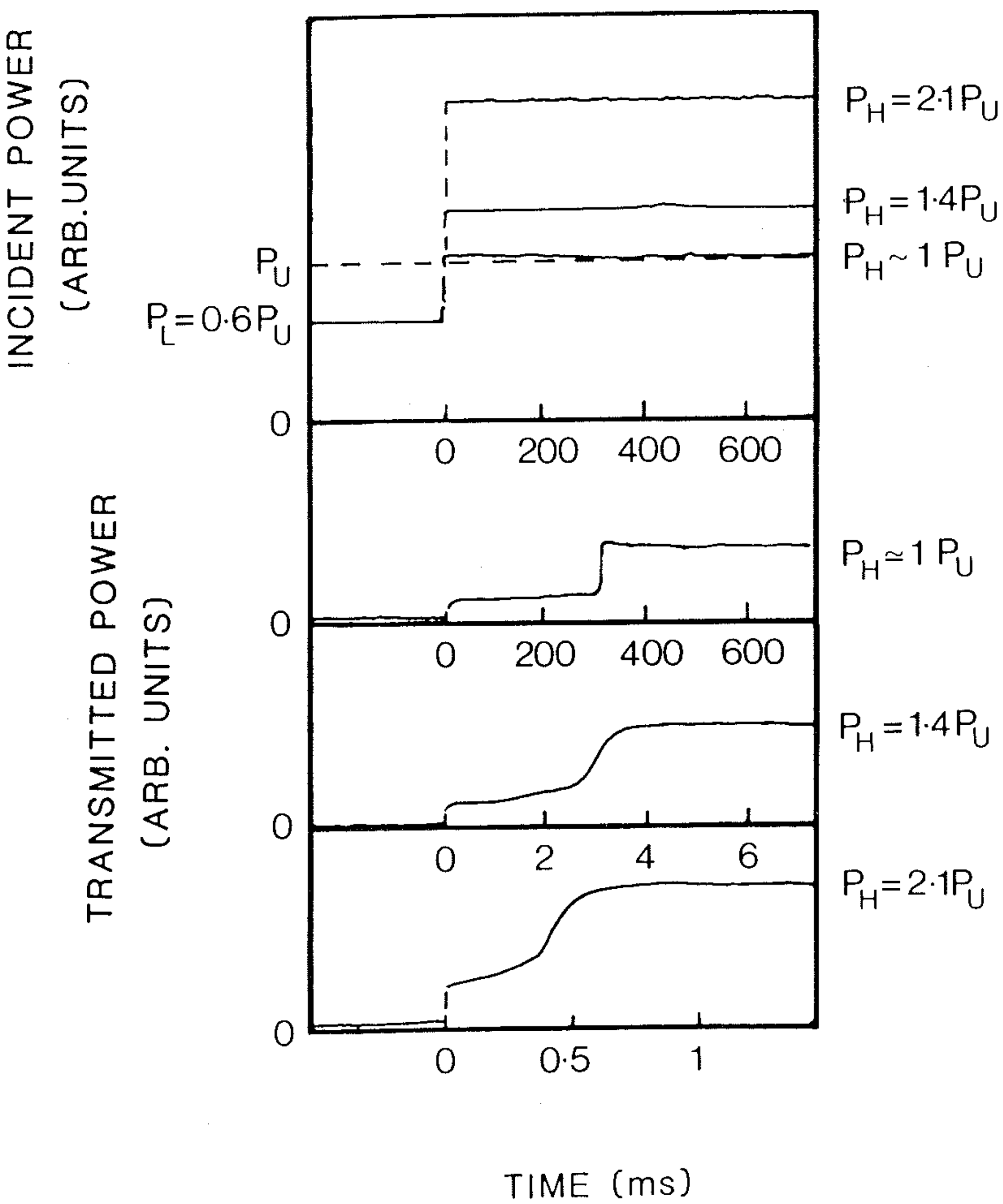

INCIDENT POWER (ARB.UNITS)
P_H=2·1P_U
P_H=1·4P_U
P_U
P_H~1 P_U
P_L=0·6P_U
0
0 200 400 600
TRANSMITTED POWER (ARB. UNITS)
P_H≃1 P_U
0
0 200 400 600
P_H=1·4P_U
0
0 2 4 6
P_H=2·1P_U
0
0 0·5 1
TIME (ms)

Fig. 2a

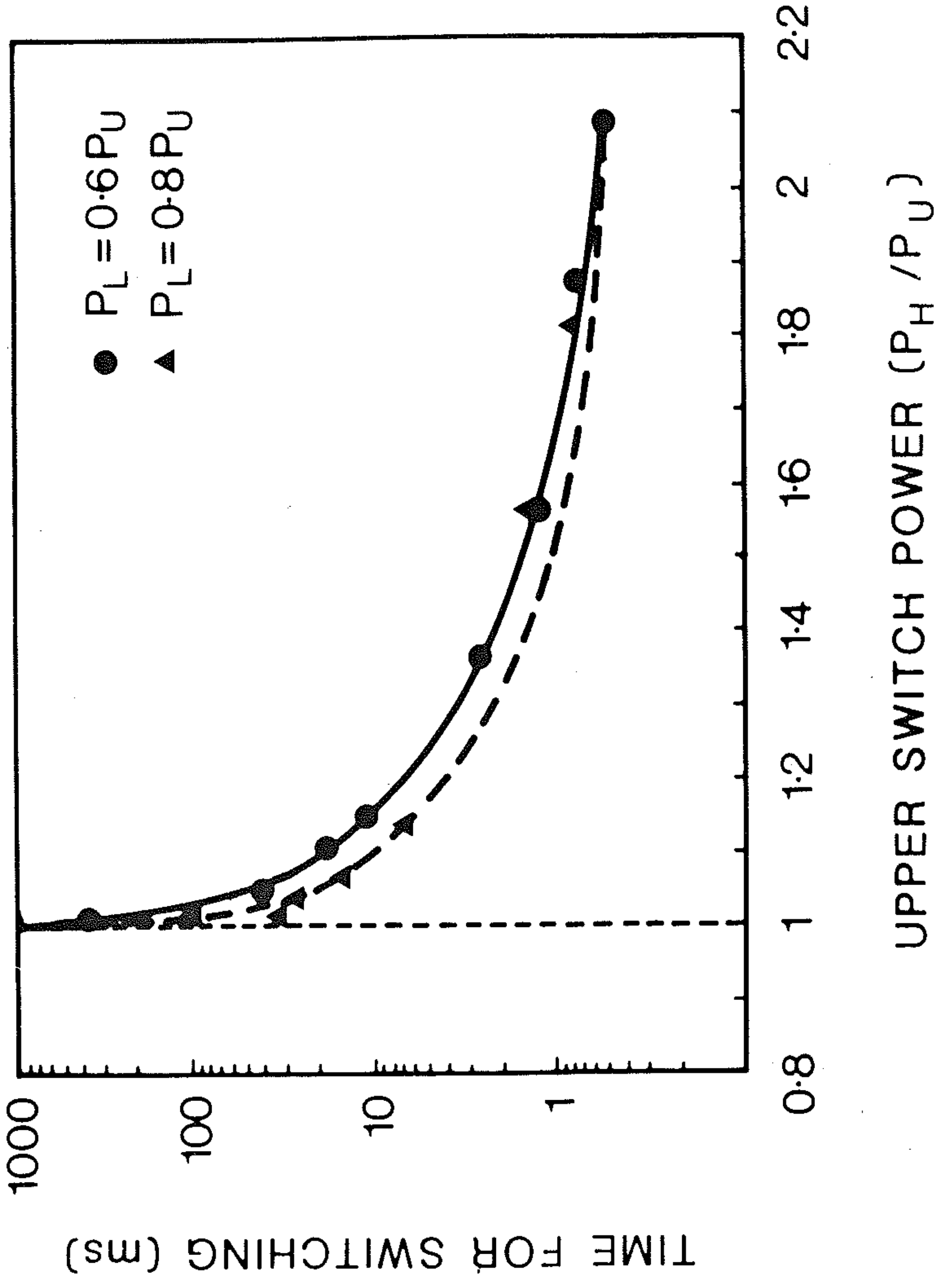

$P_L = 0{\cdot}6 P_U$
$P_L = 0{\cdot}8 P_U$
TIME FOR SWITCHING (ms)
1000
100
10
1
0·8
1
1·2
1·4
1·6
1·8
2
2·2
UPPER SWITCH POWER (P_H /P_U)

Fig. 2b

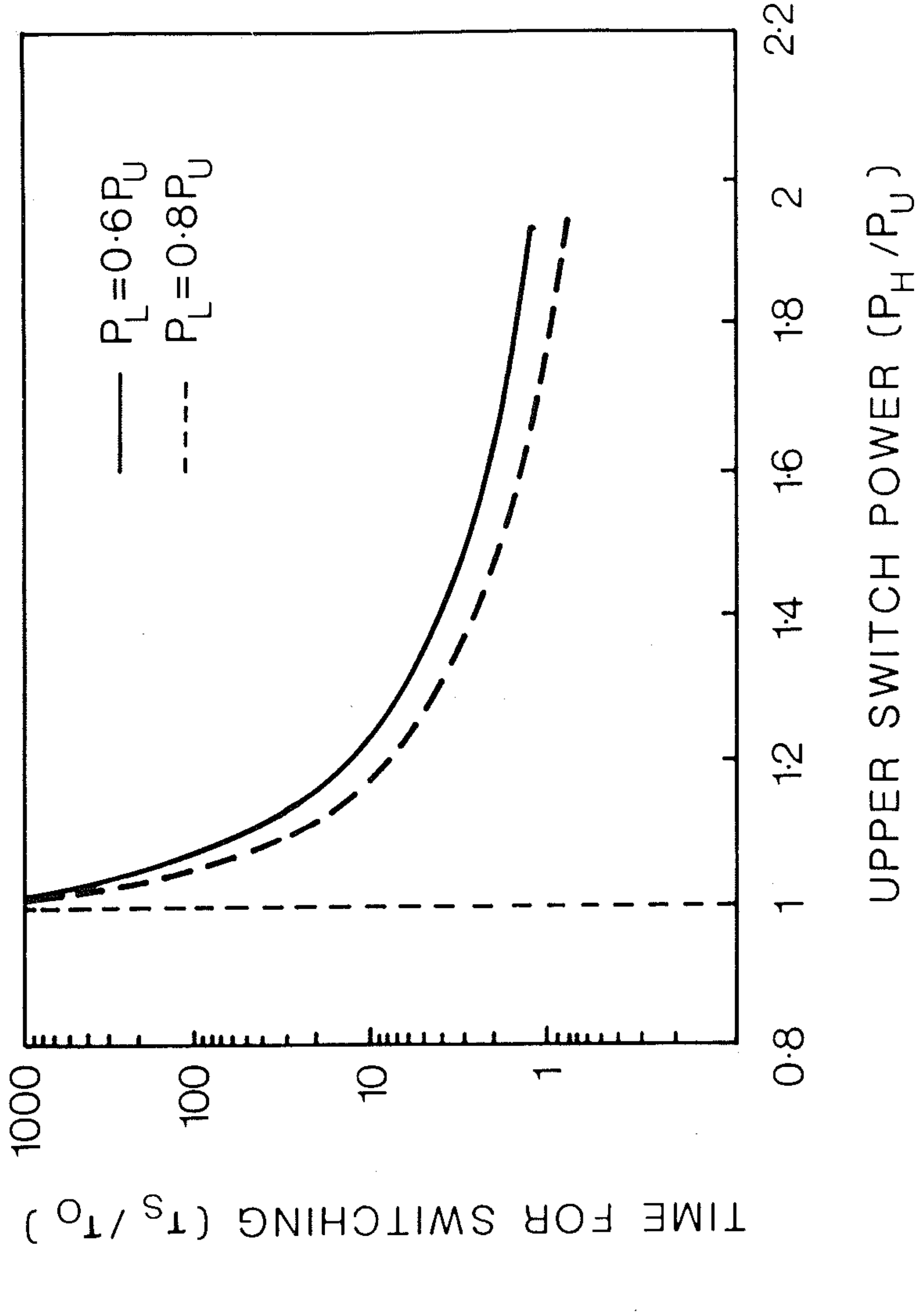

— $P_L = 0{\cdot}6P_U$
- - - $P_L = 0{\cdot}8P_U$
1000
100
10
1
0·8
1
1·2
1·4
1·6
1·8
2
2·2
UPPER SWITCH POWER (P_H/P_U)
TIME FOR SWITCHING (τ_S/τ_O)

Fig. 3

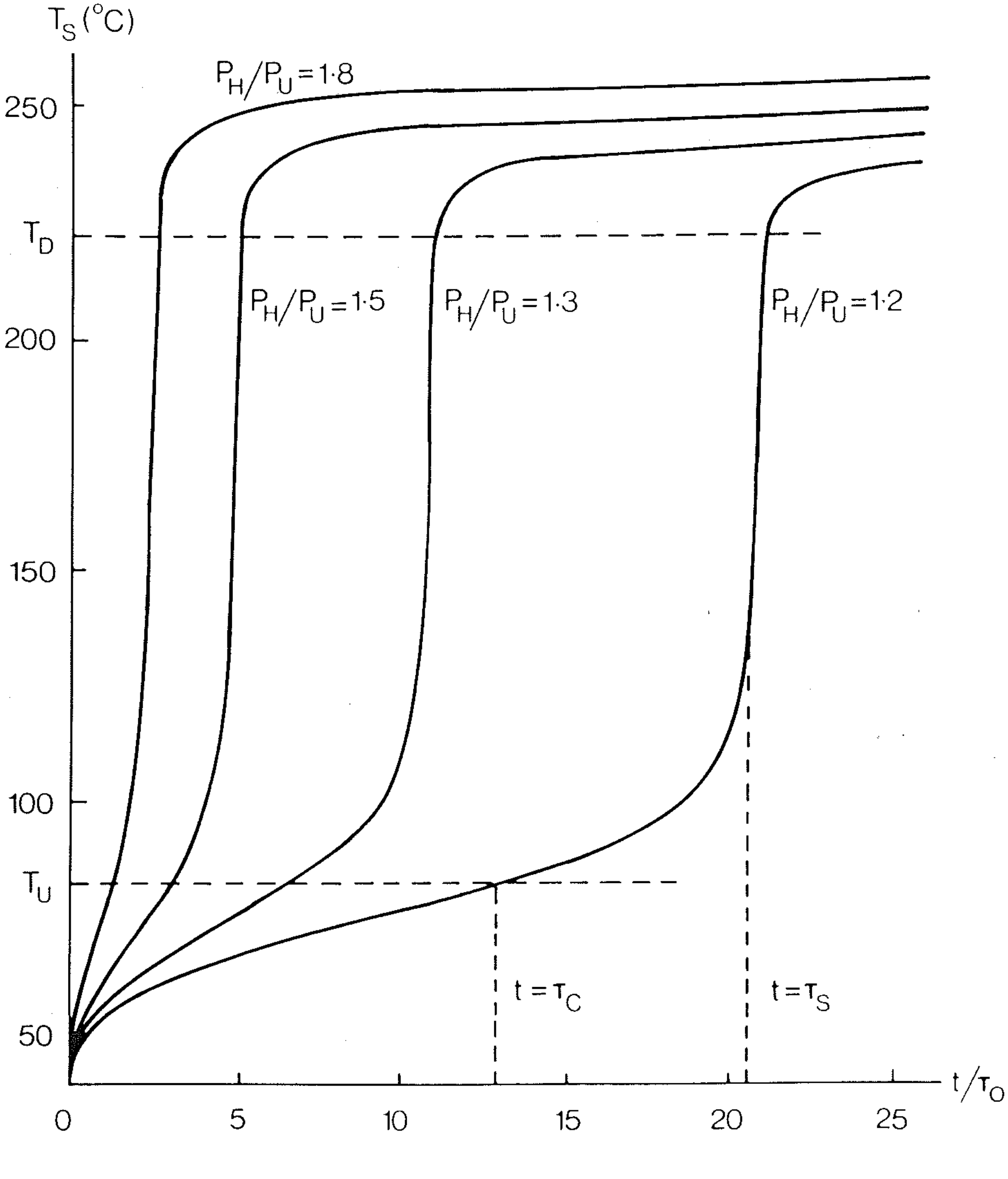

T_S (°C)
250
200
150
100
50
T_D
T_U
$P_H/P_U = 1{\cdot}8$
$P_H/P_U = 1{\cdot}5$
$P_H/P_U = 1{\cdot}3$
$P_H/P_U = 1{\cdot}2$
$t = \tau_C$
$t = \tau_S$
0
5
10
15
20
25
t/τ_O

Fig. 4.

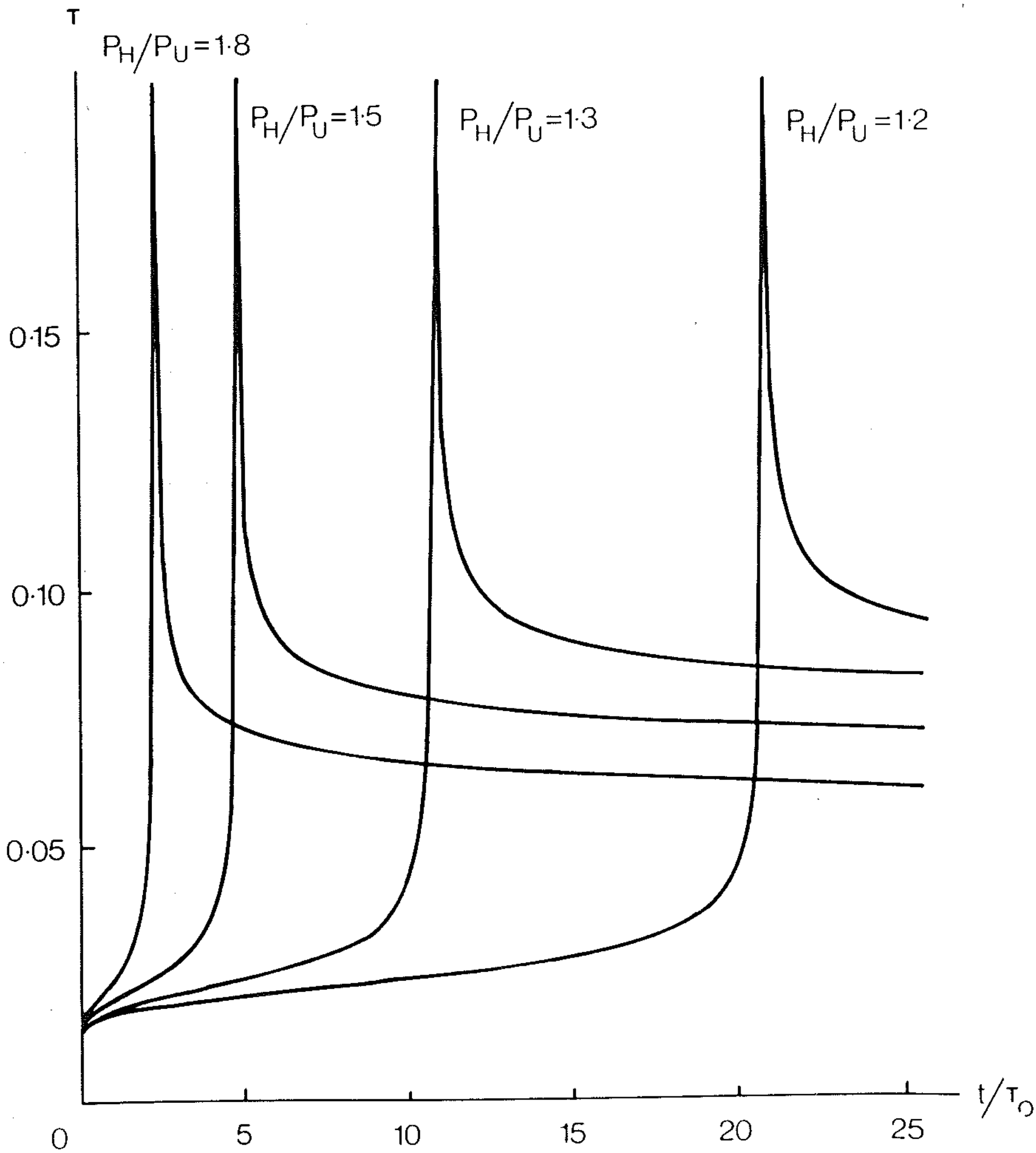

τ
$P_H/P_U = 1{\cdot}8$
$P_H/P_U = 1{\cdot}5$
$P_H/P_U = 1{\cdot}3$
$P_H/P_U = 1{\cdot}2$
0·15
0·10
0·05
0
5
10
15
20
25
t/τ_0